

Article

A Hyaluronan-Based Injectable Hydrogel Improves the Survival and Integration of Stem Cell Progeny following Transplantation

Brian G. Ballios,^{1,7} Michael J. Cooke,^{2,7} Laura Donaldson,³ Brenda L.K. Coles,⁴ Cindi M. Morshead,^{5,6} Derek van der Kooy,^{4,6,*} and Molly S. Shoichet^{2,6,*}

¹Faculty of Medicine, University of Toronto, 1 King's College Circle, Toronto, ON M5S 1A8, Canada

²Department of Chemical Engineering and Applied Chemistry, University of Toronto, 200 College Street, Toronto, ON M5S 3E5, Canada

³Division of Ophthalmology, Department of Surgery, Faculty of Health Sciences, McMaster University, 2757 King Street East, Hamilton, ON L8G 4X3, Canada

⁴Department of Molecular Genetics, University of Toronto, 1 King's College Circle, Toronto, ON M5S 1A8, Canada

⁵Department of Surgery, University of Toronto, 1 King's College Circle, Toronto, ON M5S 1A8, Canada

⁶Donnelly Centre, University of Toronto, 160 College Street, Toronto, ON M5S 3E1, Canada

⁷Co-first author

*Correspondence: derek.van.der.kooy@utoronto.ca (D.v.d.K.), molly.shoichet@utoronto.ca (M.S.S.)

<http://dx.doi.org/10.1016/j.stemcr.2015.04.008>

This is an open access article under the CC BY-NC-ND license (<http://creativecommons.org/licenses/by-nc-nd/4.0/>).

SUMMARY

The utility of stem cells and their progeny in adult transplantation models has been limited by poor survival and integration. We designed an injectable and bioresorbable hydrogel blend of hyaluronan and methylcellulose (HAMC) and tested it with two cell types in two animal models, thereby gaining an understanding of its general applicability for enhanced cell distribution, survival, integration, and functional repair relative to conventional cell delivery in saline. HAMC improves cell survival and integration of retinal stem cell (RSC)-derived rods in the retina. The pro-survival mechanism of HAMC is ascribed to the interaction of the CD44 receptor with HA. Transient disruption of the retinal outer limiting membrane, combined with HAMC delivery, results in significantly improved rod survival and visual function. HAMC also improves the distribution, viability, and functional repair of neural stem and progenitor cells (NSCs). The HAMC delivery system improves cell transplantation efficacy in two CNS models, suggesting broad applicability.

INTRODUCTION

Cell transplantation in the central nervous system (CNS) requires exogenous cells to survive and integrate into the neural circuitry, thereby restoring function. The three major barriers to successful cell transplantation in adult tissue are distribution, survival, and integration of donor cells. The co-dependency of cell survival and cell integration on transplantation efficacy has been described (Ma et al., 2011).

Targets for cell therapy in the CNS, including retina and brain, have tissue-specific challenges that must be overcome for successful treatment. In conditions such as age-related macular degeneration and retinitis pigmentosa, transplanted outer retinal cells may be able to use the remaining inner retinal circuitry, and thus photoreceptor replacement is a feasible strategy to promote functional repair of the retina (Klassen et al., 2004). Although functional restoration after subretinal cell transplantation of neonatal or embryonic stem cell (ES)-derived post-mitotic rods into adult hosts has been demonstrated (Pearson et al., 2012; Lamba et al., 2009), the majority of studies have reported relatively low survival, from 0.04% to 8% on average. Similarly, in the brain, transplanted stem cells typically show low survival of 2%–8% (Nakagomi et al., 2009). Biomaterial approaches show promise in improving the efficiency of cell transplantation.

The hyaluronan (HA) and methylcellulose (MC) (HAMC) hydrogel is injectable, minimally swelling, bioresorbable, and fast gelling (Gupta et al., 2006; Baumann et al., 2010). It was shown to be superior to a number of different natural polymers in terms of physical and biological properties, including support of stem cell progeny survival and proliferation (Mothe et al., 2013; Ballios et al., 2010). The fast-gelling properties of HAMC are key to the more uniform distribution of cells in the retina and brain compared to conventional saline delivery techniques.

The intimate relationship between cell survival and integration is investigated here with transplants of retinal stem cell (RSC)-derived rod photoreceptors. The development and characterization of adult RSC-derived rods in vitro (Ballios et al., 2012) closely resemble newborn post-mitotic rod photoreceptors in vivo (Akimoto et al., 2006), with expression of first immature (Nrl+ [Neural retina leucine zipper+]) and then mature (Rhodopsin+) rod markers in RSC progeny treated with taurine and retinoic acid (taurine/RA). Twelve-day in vitro differentiated rods ("immature" RSC-derived rods) express high levels of Nrl and low levels of Rhodopsin, whereas 28-day in vitro differentiated rods ("mature" RSC-derived rods) express high levels of both Nrl and Rhodopsin. Importantly, RSC-derived rods display electrophysiologic and functional light responsiveness in vitro that is similar to immature rod photoreceptors (Demontis et al., 2012). Transplantation of RSC-derived



photoreceptors has demonstrated functional repair in early post-natal mouse models of disease (Inoue et al., 2010).

The role of HAMC in cell survival, integration, and, ultimately, functional repair was investigated in the retina with RSC-derived rods and in the brain with neural stem and progenitor cells (NSCs). In both tissues, cells delivered in HAMC survived significantly better than those delivered in conventional buffered saline vehicles. This survival effect was mediated by cell-material interactions through CD44, the putative HA receptor, and confirmed in vivo when transplanted CD44^{-/-} RSC-derived rods no longer responded to the pro-survival effect previously observed with HAMC. In the retina, disruption of the outer limiting membrane (OLM) with DL- α -amino adipic acid (AAA) (West et al., 2008) enhanced migration/integration of cells into the host outer nuclear layer (ONL). When delivered in HAMC, these integrated cells adopted mature rod morphology, expressed mature rod markers, and improved visual function in genetically blind mice. Unexpectedly, optimization of the delivery vehicle and host environment is sufficient to promote integration of mature rods, a population of cells previously considered unsuitable for transplantation (Pearson et al., 2012; MacLaren et al., 2006).

To gain greater insight into the broad applicability for cell delivery, HAMC was investigated for the delivery of adult mouse NSCs (Morshead et al., 1994) to the brain. Significantly more cells were observed when delivered in HAMC versus artificial cerebrospinal fluid (aCSF) controls. Moreover, the depth of penetration and cell distribution were superior when NSCs were delivered in HAMC, underlining the benefit of HAMC for cell-host tissue interaction. Most important, the enhanced cell survival observed for cells delivered in HAMC versus aCSF correlated with significant behavioral recovery in the endothelin-1 (Et-1) model of stroke: only animals that had cells delivered in HAMC showed functional repair.

This study underscores the importance of the biomaterial to successful cell transplantation, where HA promotes cell survival and MC promotes cell distribution. An injectable hydrogel delivery strategy that promotes cell survival and integration of transplanted adult stem cell progeny shows promise as a strategy for cell replacement in the retina and brain for functional repair.

RESULTS

HAMC Improves Overall Survival of RSC-Derived Post-Mitotic Rods following Transplantation

RSC-derived rods at various stages of maturation were transplanted into the subretinal space of adult albino CD10 mice (Figure 1) and evaluated for survival 3 weeks post-transplantation. The survival of undifferentiated

(0-day) RSCs delivered in saline and fully differentiated (44-day) RSC-derived rods showed the poorest survival (Figure 1A), whereas the differentiated progeny (between 12 and 28 days) showed improved survival. The greatest survival was observed for the mature (28-day) RSC-derived rods transplanted in HAMC. This survival rate was significantly greater than delivery in saline, suggesting a stage-specific interaction between mature RSC-derived rods and HAMC (two-way ANOVA, vehicle and differentiation time interaction, $F(5,40) = 3.37$, $p < 0.05$). Compartmental analysis of cell distribution in host retinal tissue (Figures 1B–1D for neural retina, subretinal space, and retinal pigment epithelium [RPE] layer, respectively) using three-way ANOVA revealed a three-way interaction among differentiation time, delivery vehicle, and compartment on cell survival ($F(10,120) = 6.19$, $p < 0.05$). Committed immature RSC-derived rods (12-day differentiated) showed a greater percentage of integrated cells into neural retina compared to mature rods, regardless of delivery vehicle (post hoc analysis, $p < 0.05$) (Figure 1B). Significantly fewer cells remained in the subretinal space among immature rods (12 days) transplanted in HAMC versus saline ($p < 0.05$) (Figure 1C), demonstrating their ability to migrate into retinal tissue. Interestingly, independent of the number of days of taurine/RA differentiation, a large fraction of transplanted cells were adherent to, rather than integrated in, the RPE layer of the retina (Figure 1D), where cells were counted in the RPE compartment if they were in contact and adherent to this layer. Transplants of immature rods extended short processes following integration (Figures 1E and 1F), whereas those with mature rods in HAMC integrated into the ONL and extended processes toward the outer plexiform layer and subretinal space, compared to saline (Figures 1G and 1H). When completely undifferentiated (0-day) cells were transplanted, most cells were located in the RPE layer, and almost no cells were in the subretinal space or neural retina (Figures 1B–1D). These data are consistent with previous studies (Ballios et al., 2010).

To determine whether fusion with host cells occurred with transplanted RSC progeny, undifferentiated GFP-positive (*Actin.gfp*) RSC progeny were transplanted into adult transgenic mice that ubiquitously express mRFP (*Actin.mrfp1*). Confocal image analysis showed that GFP and mRFP signals did not overlap ($n = 4$ independent transplants; Figure S1). In addition, transplants of undifferentiated *Pax6 α -Cre* RSC progeny into *Z/EG* pups (P2) showed strong expression of the lacZ reporter in the host retina. In the case of cell fusion, GFP expression due to Cre-mediated recombination would have been expected; however, no GFP-positive cells were observed ($n = 4$ independent transplants; data not shown). On the basis of this evidence, it is unlikely that transplanted RSC progeny fused with host cells.

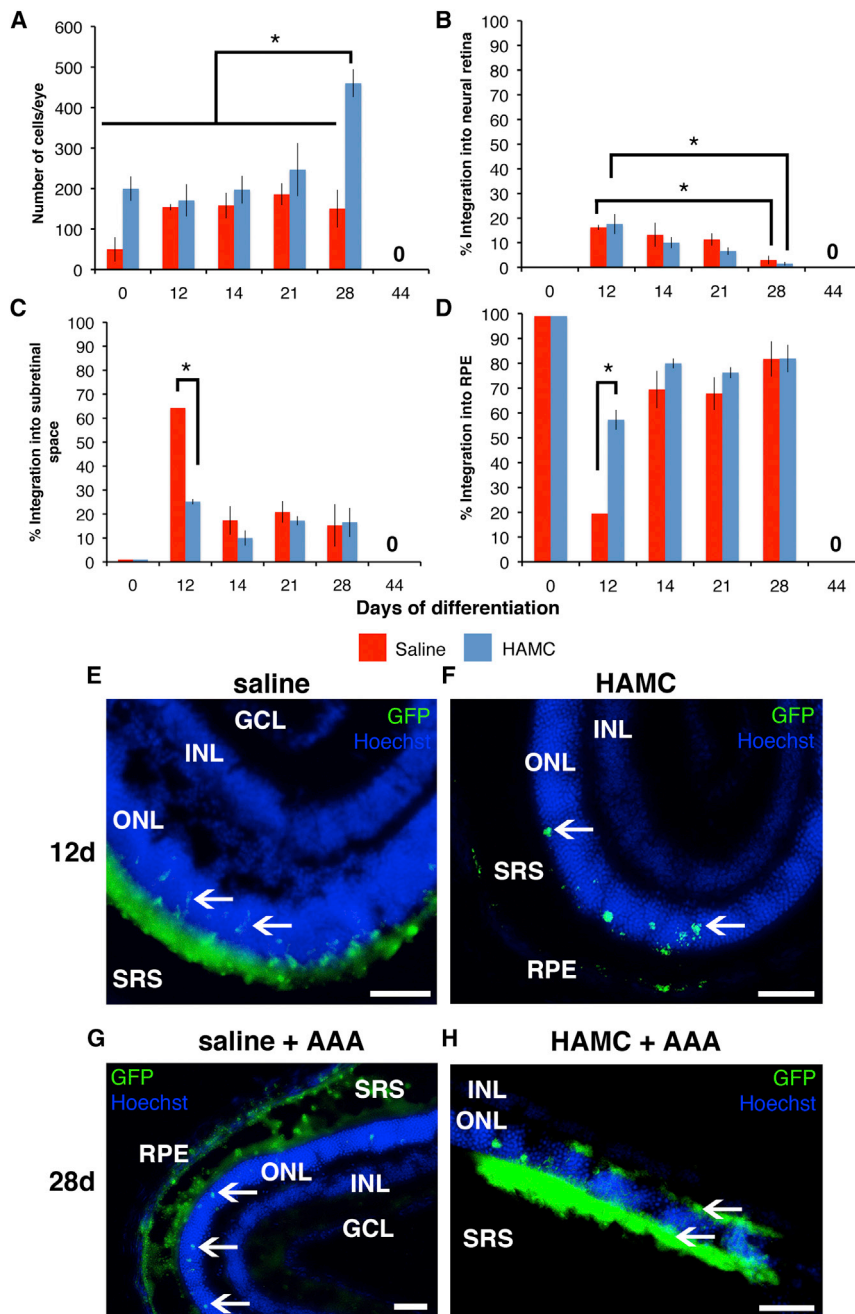


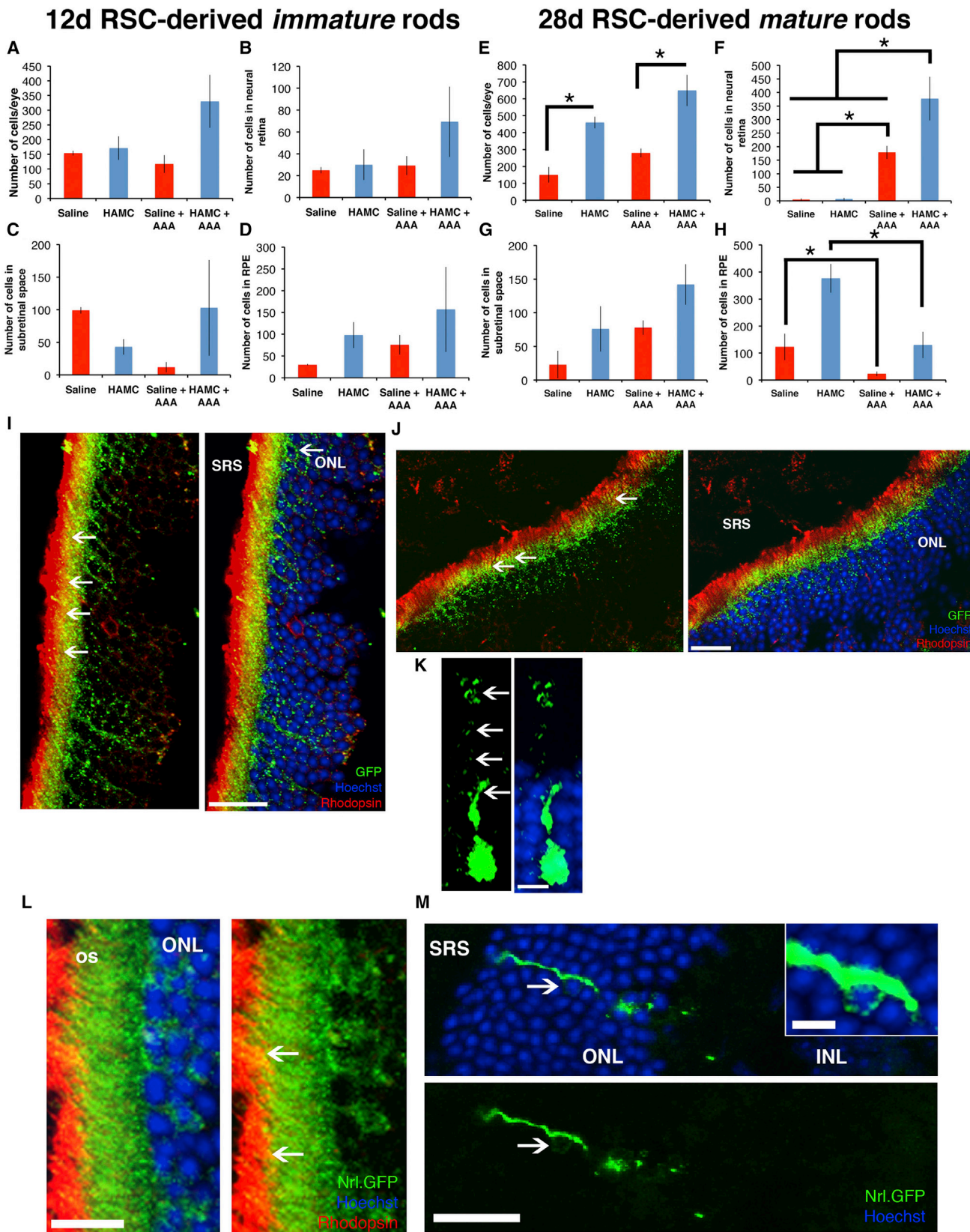
Figure 1. HAMC, an Injectable Hydrogel Matrix, Improves RSC-Derived Rod Photoreceptor Survival after Transplantation

(A–D) The absolute numbers of cells surviving in the retina of adult mice 3 weeks post-transplantation in saline versus HAMC vehicle (A). HAMC encourages the post-transplant survival of RSC-derived rods compared to saline as the maturity of the rods increases. Quantification was performed on the percentage of integrating cells (as a fraction of total cells counted in the whole eye) (B) in the neural retina, (C) in the subretinal space, and (D) adherent to the RPE layer. Immature RSC-derived rods show an ability to integrate into host neural retina independent of delivery vehicle. Mean \pm SEM of $n = 4$ –8 independent transplants are plotted; $*p < 0.05$.

(E–H) Inverted epifluorescent image of immature RSC-derived rods transplanted in saline (E) and HAMC alone (F) both show sparse integration into the ONL and extension of short processes but fail to show extensive integration and mature rod morphology (arrows). Compared to cells injected in saline+AAA (G), mature RSC-derived rods in HAMC (28-day RSC-derived rods in HAMC+AAA) (H) show patches of extensive integration into the ONL and mature rod morphology, including the extension of processes toward the outer plexiform layer and outer segments (arrows), compared to cells injected in saline. Scale bars represent 50 μ m. GCL, ganglion cell layer; INL, inner nuclear layer; ONL, outer nuclear layer; RPE, retinal pigment epithelium layer; SRS, subretinal space. See also [Figures S1–S3](#).

To understand factors that might account for the localization of cells to the RPE layer, we performed qRT-PCR analysis for the expression of photoreceptor-specific cadherin (Pr-cad) and P-cadherin (P-cad) (Figure S2). Pr-cad is expressed only in the outer segments of retinal photoreceptors (Rattner et al., 2001), whereas P-cad is typical of pigmented populations in the retina (pigmented ciliary epithelial cells, undifferentiated RSCs, and RPE cells). While immature and mature RSC-derived rods showed increased levels of Pr-cad expression in vitro relative to

undifferentiated RSCs, they did not downregulate P-cad upon differentiation and showed higher levels of P-cad expression than adult neural retina or sorted *Nrl.gfp* committed rods did. Integrated rods did not express P-cad, and cells adhering to the RPE layer did not express RPE65 yet did express P-cad (Figure S2). Together, these data suggested that these donor cells were not RPE cells, but maintained expression of P-cad post-transplantation, which limited their integration into the neural retina.



(legend on next page)



We sought to determine whether tissue immune response in the retina varied depending on the cell delivery vehicle. Injections of immature and mature cells showed a higher immune response in saline than in HAMC (Figure S3), as measured by the number of CD68-positive activated macrophages within the neural retina following injection. Mature (28-day) cells delivered in HAMC had significantly fewer CD68+ cells/retina than immature (12-day) cells delivered in saline. Post hoc analysis revealed that 28-day differentiated cells in saline showed significantly fewer CD68+ cells/retina compared to 12-day differentiated cells in saline (Figure S3) ($p < 0.05$), suggesting that tissue immune response is correlated with differentiation stage of the transplanted cells. Interestingly, HAMC has also been previously shown to attenuate the inflammatory response in the CNS (Austin et al., 2012), and thus we ascribed the trend toward decreased number of CD68+ cells present after cell transplantation in HAMC versus saline to the HA in the HAMC hydrogel.

Disruption of the Outer Limiting Membrane Enhances Integration of Immature and Mature RSC-Derived Rods

Adult retinal tissue poses significant barriers to integration of donor rods. One of these barriers is the presence of the OLM, which restricts the ability of donor cells to migrate into the retina following subretinal transplantation. Pharmacological disruption of the OLM is achieved using a transiently acting gliotoxin (i.e., AAA) (West et al., 2008). This disruption is reversible, with re-establishment of the OLM and normal retinal cytoarchitecture. Pre-treatment with AAA combined with transplantation of immature

(Figures 2A–2D) or mature (Figures 2E–2H) RSC-derived rods in HAMC resulted in higher survival and integration of cells into the neural retina than delivery of cells in either saline or HAMC in the absence of AAA. Total cell survival analysis showed a differentiation stage-specific positive interaction of mature RSC-derived rods with HAMC (three-way ANOVA, interaction between vehicle and differentiation time, $F(1,36) = 8.08$, $p < 0.05$) (Figures 2A and 2E). The effect of AAA on cell survival was independent of the effects of vehicle or differentiation time (statistical interaction, $p > 0.05$). Thus, AAA acted specifically on removing barriers to neural retinal integration rather than overall cell survival. Of note, mature cell survival in HAMC (with or without AAA) was significantly greater than immature cell survival in HAMC ($p < 0.05$) (compare Figures 2A and 2E). Overall, our analyses demonstrated that the more mature cells delivered in HAMC+AAA showed the greatest survival relative to other delivery conditions ($p < 0.05$).

Analysis of cell survival reinforced the hypothesis that cell survival factors, such as differentiation stage or delivery in HAMC, can act with integration-promoting factors to improve survival specifically in the neural retina (four-way ANOVA, interaction of time, vehicle, AAA treatment, and compartment; $F(2,69) = 7.28$; $p < 0.05$) (Figures 2B–2D and 2F–2H). Multiple group comparison revealed that survival in the neural retina was significantly higher for mature versus immature cells for saline+AAA or HAMC+AAA delivery ($p < 0.05$) (compare Figures 2B and 2F). Post hoc analysis showed that more mature (28-day) cells delivered in HAMC+AAA had the greatest potential for integration into the neural retina across all conditions ($p < 0.05$) (Figure 2F). In the case of mature RSC-derived

Figure 2. Disruption of the Outer Limiting Membrane Combined with HAMC Delivery Reveals the Integration Potential of Mature RSC-Derived Rod Precursors

(A–H) Compartmental analysis of (A–D) immature (12-day differentiation) or (E–H) mature (28-day differentiation) RSC-derived rod precursors surviving 3 weeks post-transplantation following delivery in saline, HAMC, saline+AAA, and HAMC+AAA. The absolute numbers of surviving cells are stratified depending on whether they localize to neural retina, subretinal space, or the RPE layer. Application of AAA to modify the host retina significantly increases the number of surviving RSC-derived rod progeny when combined with delivery in HAMC. (I) Confocal image analysis shows mature RSC-derived rods transplanted in optimum conditions (HAMC+AAA) extend Rhodopsin-positive outer segments (yellow, arrowheads in left panel) toward the subretinal space similar to previous reports of integrated photoreceptors (Pearson et al., 2012). Cell bodies completely surrounded by GFP were counted (arrows, right panel). (J) Endogenous rod outer segments (red) are separately identified from the outer segments of integrated cells (yellow, arrows). Nuclei/GFP/Rhodopsin merge is shown on the left, and GFP/Rhodopsin merge is shown on the right. (K) The majority of rod photoreceptors integrated as clusters of cells; however, rare single cells elaborate processes into the subretinal space (arrowheads). (L) Transplants of dissociated retinal cells from P4 *Nrl.gfp(+/+)* mice into wild-type adult retina ($n = 6$) demonstrate rod integration consistent with previous reports (MacLaren et al., 2006). Where clusters of cells integrate into the ONL, morphology is strikingly similar to integrated mature RSC-derived rods, including the extension of Rhodopsin-positive outer segments (yellow, arrowheads). (M) A single integrated *Nrl.gfp(+/+)* rod photoreceptor showing elongated morphology similar to single mature RSC-derived rods (nucleus, arrowhead and inset).

Scale bars represent (I–J) 20 μm , (K) 5 μm , (L) 10 μm , and (M) 20 μm (inset 5 μm). OS, outer segments; GCL, ganglion cell layer; INL, inner nuclear layer; ONL, outer nuclear layer; RPE, retinal pigment epithelium layer; SRS, subretinal space. Mean \pm SEM of $n = 4$ –6 independent transplants; * $p < 0.05$.

rods, the application of AAA resulted in more cells in the desired neural retina at the expense of cells in the RPE layer ($p < 0.05$) (Figures 2F and 2H).

The highest numbers of cells integrating into the neural retina were mature rods delivered in HAMC to mouse retinæ pre-treated with AAA (380 ± 80 , or 2.4%–4.3% of cells injected). This result is surprising because, previously, early post-mitotic rods isolated from P4 *Nrl.gfp* mice showed integration at a lower survival rate (0.04%–0.13%) (MacLaren et al., 2006). We have shown that by modifying the host retinal environment to remove barriers to migration, mature rod precursors have greater potential to achieve more efficient integration. Transplants of integrated mature rods adopt typical rod photoreceptor morphology (Figure 1H), including the extension of Rhodopsin-positive outer segments (Figures 2I–2K). These cells also appear to extend processes toward the outer plexiform layer, where rods typically form connections with bipolar interneurons (Figure 1H). The morphology observed with mature RSC-derived rod transplants was strikingly similar to transplants of P4 *Nrl.gfp* rod precursors into adult retina ($n = 4$ independent transplants; Figures 2L and 2M). Interestingly, our RSC-derived rod transplants exhibited similar patch-like integration pattern and staining to those of integrated post-mitotic rods, despite having different relative intensities of cell body versus process immunostaining (Pearson et al., 2012; MacLaren et al., 2006). Our images also show the extension of a GFP-bright, mature, Rhodopsin-positive outer segment “brush border,” an essential element of mature rod photoreceptor morphology. The data suggest that physical integration barriers, such as the OLM, are critical factors limiting integration.

HAMC Directly Promotes RSC-Derived Rod Survival through CD44-Mediated Inhibition of Apoptosis

Cell survival and phenotype in HAMC were studied using mature RSC-derived post-mitotic rods. RSC progeny were differentiated either in the presence of taurine/RA (rod-induction) or 1% fetal bovine serum (FBS) (pan-retinal differentiation). At 28 days, induction factors were removed, and the cells were exposed either to HAMC reconstituted in serum free media (SFM) or to SFM alone for 7 days. Post-mitotic rods showed significantly higher survival over 7 days when cultured in HAMC relative to SFM alone (Figure 3A). No change in mature photoreceptor phenotype, as determined by Rhodopsin expression, was noted over 7 days of culture (Figure 3B). The observation that RSC-derived rods maintained their post-mitotic phenotype in the absence of taurine/RA suggests that they are terminally differentiated (Figure 3C). By contrast, pan-retinal cultures derived in 1% FBS, which include a significant number of multipotent proliferative progenitors (Ballios

et al., 2012), showed similar overall in vitro survival in both HAMC and SFM alone (Figure S4). There was no difference in the proportions of the Rhodopsin-positive population. Thus, the direct effect of HAMC on cell survival appears specific to the population of post-mitotic RSC-derived rods.

In order to determine the component of HAMC responsible for the survival effect noted in the post-mitotic rods, cells were cultured in HA and MC separately. HA and HAMC had pro-survival effects, whereas cells cultured in MC and SFM showed similar cell death rates (Figure 4A). We hypothesized that HA supports cell survival through a direct CD44-mediated interaction with donor cells. CD44 is the putative HA receptor, and its activation is important in cell survival pathways in other tissues. Mature RSC-derived rods were found to express CD44 both by immunocytochemistry (ICC) and qRT-PCR (Figures 4B and 4C). Just as RSC-derived rods maintain progenitor levels of P-cad expression during differentiation in vitro, they continue to express high expression of CD44, unlike mature rod photoreceptors in adult retina (Sarthý et al., 2007; Chaitin et al., 1994). The levels of CD44 gene expression were maintained over more than 7 days in HA or MC-containing mixtures, demonstrating that the medium itself did not affect gene expression. Additional evidence for the pro-survival effect of HA in HAMC was achieved by quantification of activated caspase-3 levels in these cultures. Significantly greater levels of apoptosis were observed with RSC-derived rods cultured in non-HA-containing, compared to HA-containing, hydrogels ($p < 0.05$) (Figure 4D).

To test the hypothesis that the pro-survival action of HA was through the CD44 receptor, we cultured RSC-derived rods from CD44^{-/-} mice. The pro-survival effect observed with HAMC for CD44^{+/+} rods was lost with CD44^{-/-} rods over 7 days. Cell death rates were not significantly different from those of cells cultured in MC and SFM only (Figure 4E). Importantly, the CD44^{-/-} cells were identical to wild-type RSC-derived rods in terms of their Rhodopsin-positive phenotype (Figure 4F) and differed only in their expression of CD44.

Factors Enhancing Integration Are Dependent on Pro-Survival Signals In Vivo for Improvement of Transplant Efficacy

To probe the interplay between survival and integration of the RSC-derived rod donor population in the adult retina, it was necessary to dissociate these two effects. Transplants of immature and mature RSC-derived rods in optimal cell survival or integration conditions (HAMC+AAA) were performed using cells derived from CD44^{-/-} mice. On the basis of the in vitro studies, the loss of CD44 should eliminate the pro-survival effect of HAMC on the transplanted cells in vivo. Significantly fewer CD44^{-/-} RSC-derived rods

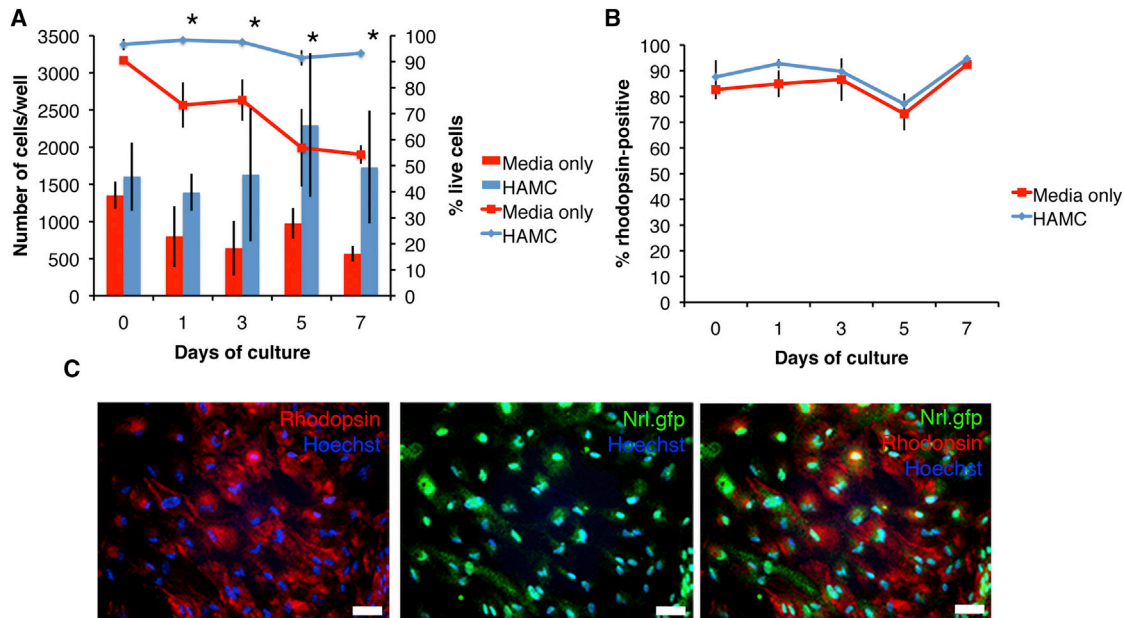


Figure 3. HAMC Promotes the Survival of Mature RSC-Derived Rods In Vitro

(A) Absolute numbers (bars) and percentage survival (line plot) of mature RSC-derived rods (28-day differentiated, > 95% Nrl+/ Rhodopsin+) maintained for 7 days in culture in either HAMC reconstituted in serum-free medium (SFM) or SFM alone. Percentage survival in HAMC is significantly greater than in media (two-way ANOVA, interaction between mixture composition and culture time, $F(4,25) = 3.44$, $p < 0.05$; Tukey-Kramer post hoc, $p < 0.05$).

(B) Rhodopsin expression is maintained in the absence of taurine/RA induction factors regardless of culture in HAMC or SFM alone (interaction of mixture composition and culture time was not significant, $F(4,25) = 0.18$, $p > 0.05$; no main effect of mixture composition).

(C) Mature RSC-derived rods express Nrl (cytoplasmic GFP) and Rhodopsin. Scale bar represents 50 μm . Mean \pm SEM of $n = 3$ independent transplants are plotted; * $p < 0.05$.

See also [Figure S4](#).

survived in the retina when injected with HAMC+AAA—our optimized condition that showed the greatest level of CD44^{+/+} cell survival (two-way ANOVA, vehicle and differentiation time interaction, $F(4,45) = 10.53$, $p < 0.05$) ([Figures 5A](#) and [5E](#)).

The decreased survival of CD44^{-/-} cells was observed in the neural retina, subretinal space, and RPE layer ([Figures 5B–5D](#) and [5F–5H](#)). In the absence of functional CD44, cell integration into neural retina or RPE layers—despite removal of the OLM by AAA—followed the same profiles for transplantation in saline without AAA ($p > 0.05$; [Figures 5B](#), [5D](#), [5F](#), and [5H](#)). Analysis of cell integration across all retinal compartments ([Figures 5B–5D](#) and [5F–5H](#)) shows that the three-way interaction of vehicle, differentiation time, and compartment was significant ($F(8,111) = 27.49$, $p < 0.05$). Of note, multiple comparisons demonstrate a significant reduction in overall survival of both immature ([Figures 5B–5D](#)) and mature ([Figures 5F–5H](#)) CD44^{-/-} RSC-derived rods compared to CD44^{+/+} RSC-derived rods transplanted in HAMC+AAA ($p < 0.05$). This experiment separates the roles of survival and integration on overall transplant efficacy. While the OLM barrier is a ceiling to

maximum cell survival, pro-survival signals are critical to long-term cell viability in vivo, independent of the compartment in which cells localize after transplantation.

Transplantation of RSC-Derived Rod Photoreceptors Improves Visual Function in Genetically Blind Mice

To test the ability of RSC-derived rod photoreceptors to enhance visual function, we transplanted our optimal mature RSC-derived rods in HAMC in host animals that have an intact retina similar to wild-type animals but that fail to show pupillary light reflex, do not entrain light/dark cycles, and do not respond to light (*Gnat1*^{-/-}, *CngA3*^{-/-}, *Opn4*^{-/-}) (triple knockout, TKO mice) ([Hattar et al., 2003](#)). Any response from these retinæ would only arise from a transplanted cell population, and outcomes related to effective tissue integration and donor cell function could be evaluated without the complication of a degenerating host environment. The pupil responses of uninjected wild-type mice and TKO mice that had received 28-day differentiated RSC-derived rods in HAMC+AAA into one eye and sham injections (HAMC+AAA without cells) into the other ($n = 16$) were examined at various

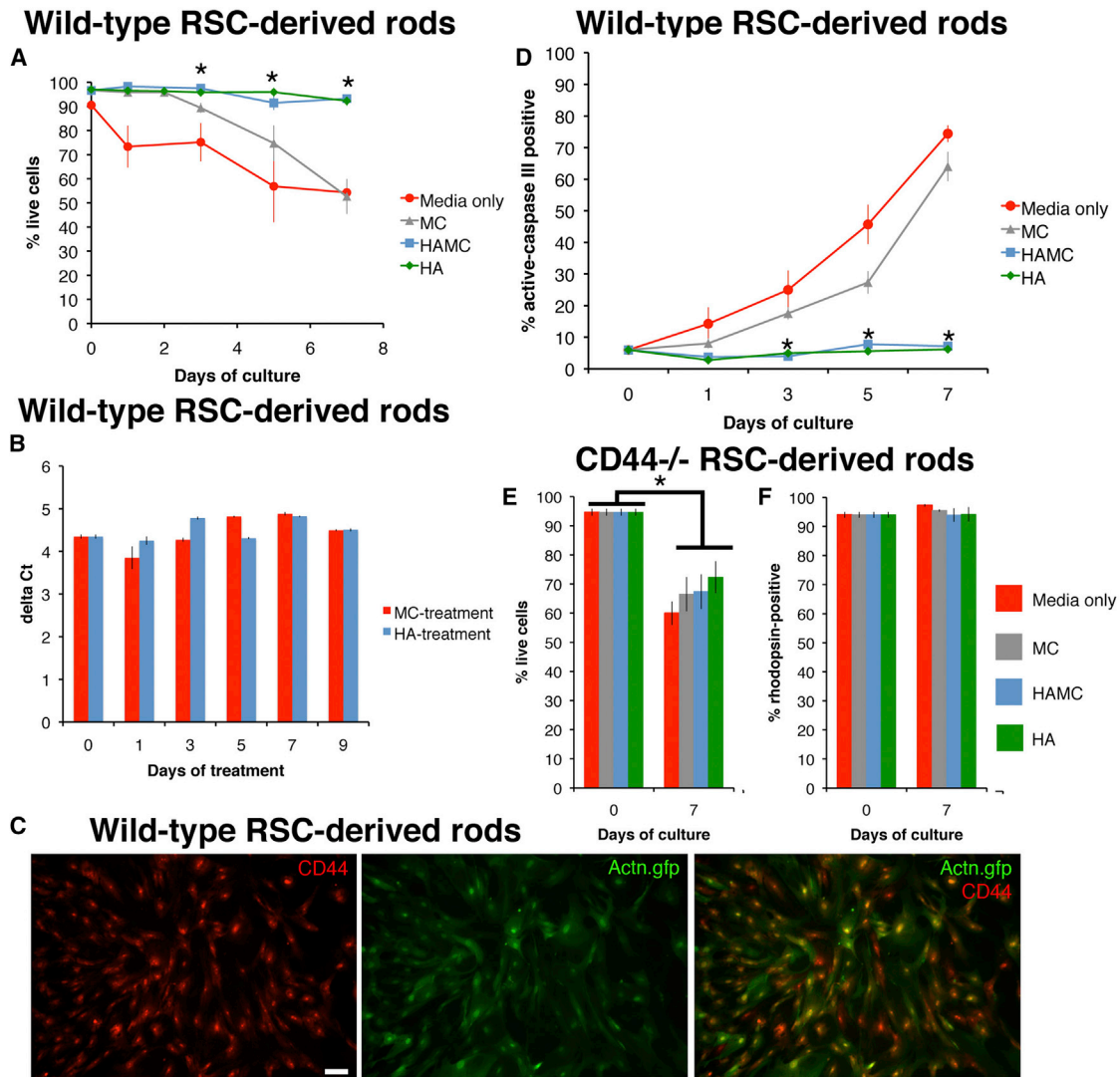


Figure 4. CD44 Mediates the Direct Survival Effect of HAMC on RSC-Derived Rods In Vitro

(A) Percentage survival of mature RSC-derived rods (assayed with ethidium homodimer-1) cultured in HAMC and its individual components (HA and MC) demonstrates that only those mixtures containing HA show a significant pro-survival effect compared to non-HA-containing mixtures (two-way ANOVA, interaction effect of culture time and mixture composition on rod survival, $F(12,102) = 10.33$, $p < 0.05$; Tukey-Kramer post hoc, $p < 0.05$).

(B) CD44 expression by qRT-PCR remains constant regardless of culture in HA- or MC-containing mixtures.

(C) Mature RSC-derived rods express CD44 by immunocytochemistry, which co-localizes with GFP consistent with surface localization.

(D) Staining for activated caspase III suggests cell death occurs primarily through apoptosis without HA-CD44 interaction in non-HA-containing mixtures (interaction of culture time and mixture on rod numbers, $F(12,96) = 37.78$, $p < 0.05$).

(E) When mature CD44^{-/-} RSC-derived rods are cultured for 7 days, cell survival is decreased by the same proportion compared to day 0, independent of mixture composition. Two-way ANOVA showed a main effect of culture time ($F(1,40) = 258.92$, $p < 0.05$), but no effect of mixture composition ($F(3,40) = 0.71$, $p > 0.05$) and no interaction effect ($F(3,40) = 2.12$, $p > 0.05$) on rod survival.

(F) CD44^{-/-} RSC-derived rods maintain Rhodopsin expression, suggesting that the absence of CD44 does not affect cell phenotype (no interaction effect, $F(3,40) = 0.58$, $p > 0.05$; no main effects of time or mixture composition) Scale bar represents 100 μm . Mean \pm SEM of $n = 3$ independent transplants are plotted; * $p < 0.05$.

light intensities. Wild-type pupils showed responses consistent with previous studies (Figures 5I and 5S) (MacLaren et al., 2006). Sham-injected TKO eyes showed no pupillary

light response, while those that received RSC-derived rods showed a significant improvement in pupillary constriction at higher intensities ($p < 0.05$), to a maximum response

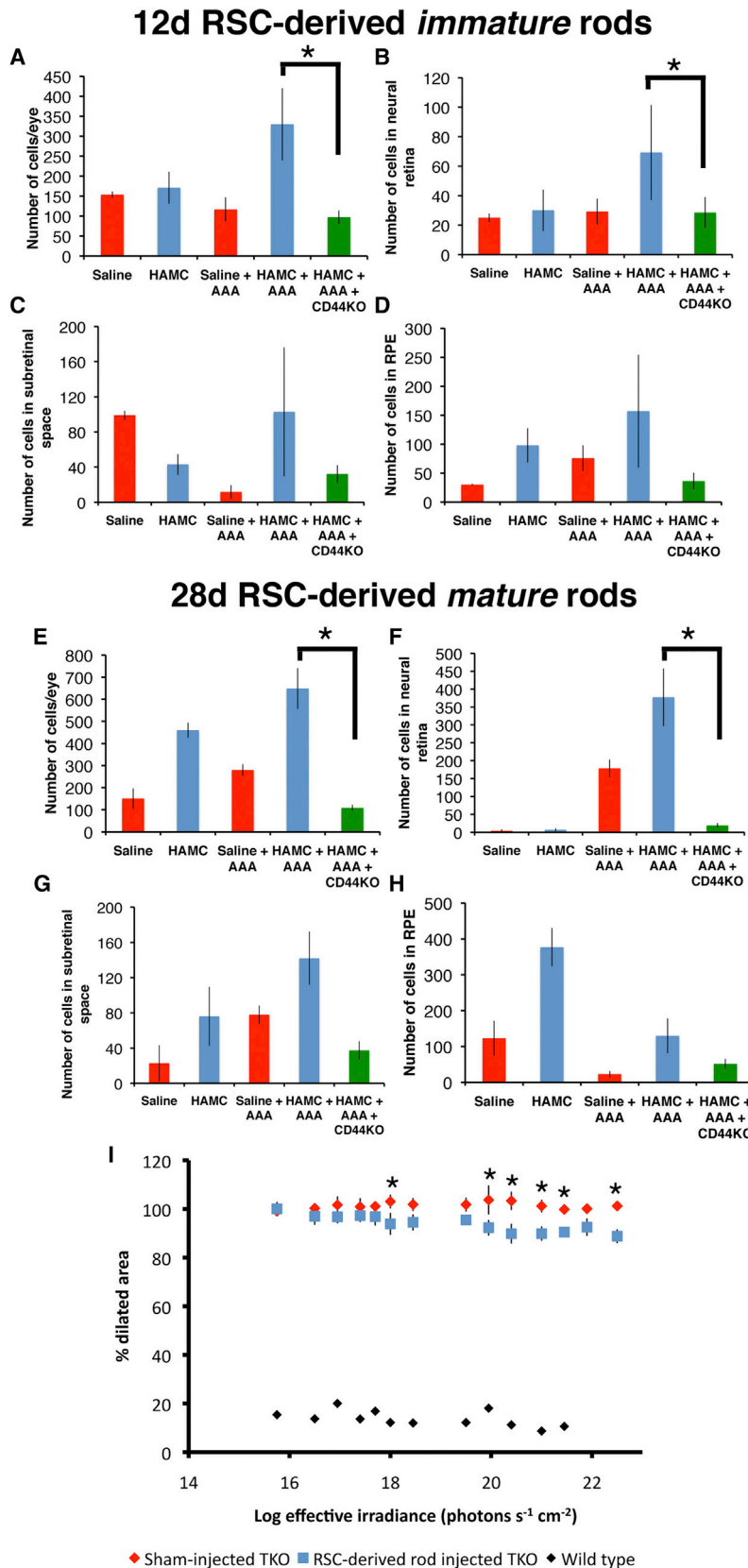


Figure 5. HAMC-CD44 Interaction Is Critical for RSC-Derived Rod Survival and Integration Ability In Vivo, and RSC-Derived Rods Show Functional Visual Recovery in Genetically Blind Mice

(A–H) Compartmental analysis of (A–D) immature (12-day differentiation) and (E–H) mature (28-day differentiation) RSC-derived rod precursors following delivery in various conditions. Immature or mature CD44^{-/-} RSC-derived rod precursor transplantation in HAMC+AAA shows significantly decreased cell survival and suggests the pro-survival effect of HAMC on donor cells is necessary for their ultimate survival and ability to integrate into host retina. Mean ± SEM of n = 4–6 independent transplants are plotted; *p < 0.05.

(I) Wild-type pupillary light response is consistent with previous reports (MacLaren et al., 2006) and shows 80% constriction in pupillary area over the entire range of irradiances tested. Pupillary light response was measured in TKO mice that received 28-day CD44^{+/+} RSC-derived rods in HAMC+AAA in one eye and a sham injection (HAMC+AAA without cells) into the other. Note the pupillary response identified at high effective irradiances in the cell-injected eye compared with no response in sham-injected eyes at any intensity (F(13,420) = 3.48, p < 0.05). Mean ± SEM of n = 16 mice; *p < 0.05. See also Figure S5.

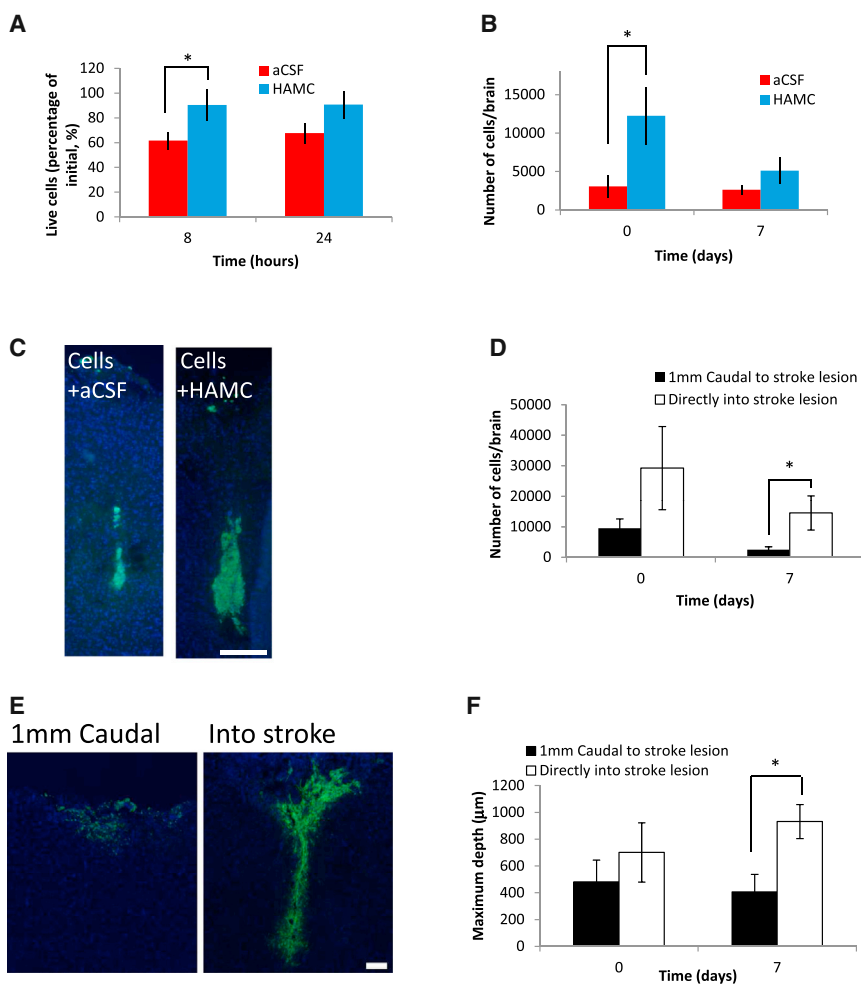


Figure 6. HAMC Increases the Number of Live NSCs Transplanted into Uninjured Mouse Brain

(A) Prior to transplantation, the effect of storing the cells on ice was monitored over time and compared to time 0. After 8 hr, there were significantly more live YFP+ NSCs in HAMC than in aCSF ($p = 0.04$, $n = 7$). This trend persisted to 24 hr but was not significantly different ($p = 0.06$, $n = 7$).

(B) Mice transplanted with NSCs in HAMC have significantly more YFP+ live NSCs in the brain at time 0 compared to those transplanted with cells in aCSF ($p < 0.05$, $n = 7$). This trend of more NSCs in the brain when delivered in HAMC than in aCSF persists to 7 days; however, the difference is not significant at 7 days ($n = 4-6$).

(C) Representative images of transplanted YFP cells show more NSCs in the mouse brain when injected in HAMC versus aCSF. Scale bar represents 200 μm .

(D) Quantification demonstrates more GFP+ live NSCs in the stroke site versus the uninjured tissue at both 0 and 7 days; however, the difference is only significant at 7 days ($p < 0.05$, $n = 6$).

(E) Representative images show that animals transplanted with cells suspended in HAMC directly into the stroke site (4 days after stroke injury) appear to have a greater number of cells compared to those transplanted with cells in HAMC 1 mm caudal to the injury ($n = 6$). Scale bar represents 100 μm .

(F) NSCs injected in HAMC directly into the stroke lesion penetrate to greater depths than those transplanted 1 mm caudal to the injury site; however, there is only a significant difference 7 days after transplantation ($p < 0.05$, $n = 6$).

For all graphs, mean \pm SEM are plotted, n independent transplants.

See also [Figure S6](#).

of approximately 10% constriction, demonstrating vision improvement ([Figure 5I](#)). Our results are similar in magnitude to the 10%–20% improvement seen after cell transplantation into models of active retinal degeneration ([MacLaren et al., 2006](#)), thereby validating the benefit of RSC-derived rod photoreceptor transplantation in HAMC+AAA in the TKO model.

HAMC Improves NSC Viability

To understand the benefit for cell transplantation more generally, we investigated HAMC delivery of NSCs into non-injured and stroke-injured adult mouse brain. As with RSC progeny, NSCs also express CD44 at both the mRNA and protein levels ([Figure S6A](#)), suggesting that the direct pro-survival effect of HAMC would also be observed with NSCs. We evaluated NSC survival in vitro

at 8 and 24 hr. After 8 hr, 60% of NSCs in aCSF were viable compared to 90% in HAMC, demonstrating a significant pro-survival effect of HAMC ($p < 0.05$; [Figure 6A](#)). At 24 hr, there was a trend toward greater cell survival in HAMC versus aCSF, but no significant difference. Since all NSCs were injected within 8 hr of preparation, the number of transplanted cells in HAMC ($\sim 126,000$) was significantly greater than those transplanted in aCSF ($\sim 87,000$). Thus, the beneficial pro-survival effect of HAMC in vitro likely affects in vivo results.

In vivo survival was quantified immediately after transplantation into uninjured mouse brains (0 days) and at 7 days for equal numbers of NSCs suspended in aCSF or HAMC. Immediately after injection, mice transplanted with NSCs in HAMC had significantly more cells than those transplanted in aCSF ($p < 0.05$; [Figure 6B](#)). After



7 days, we observed more cells after delivery in HAMC versus aCSF, but the difference was not significant ($p = 0.12$). Notably, 86% of mice (i.e., 6 of 7) transplanted with NSCs in HAMC had cells present after 7 days, whereas only 57% (4 of 7) had cells present at 7 days when transplanted in aCSF (Figure S6B). Immediately after injection, cells transplanted in HAMC appeared to be distributed throughout the injection site, whereas cells in aCSF appeared localized mainly dorsally, possibly due to backflow following injection (Figure 6C). Quantification of the injection depth showed that NSCs delivered in HAMC remained deeper within the brain tissue than did cells delivered in aCSF, although this difference was insignificant (data not shown). Thus, HAMC had a pro-survival effect on NSCs in vitro and promoted greater cell distribution in vivo.

Transplantation Directly into the Stroke Injury Increases Cell Survival

To test transplantation efficacy, the Et-1 mouse model of stroke was employed. Et-1 is a chemically induced stroke previously described in the literature (Wang et al., 2013). Cells were transplanted 4 days after injury to ensure neuron cell death in the resulting tissue cavity while at the same time providing a sub-acute model, which has clinical relevance. NSCs delivered in HAMC were injected either at the site of the injury or 1 mm caudal to the injury site. Interestingly, significantly more cells were observed in the brain when injected into the injury site versus caudal at 7 days post-transplantation ($p < 0.05$) (Figures 6D, 6E, and S6B). This greater number of cells in the injury site correlated with greater depth of tissue penetration when NSCs were delivered into the injury site than caudal to the site at 7 days ($p < 0.05$; Figure 6F). The greater number and deeper penetration observed may be due to the greater tissue volume available for NSCs in the stroke-injury site.

NSCs Show Improved Survival in the Adult Brain after Stroke Injury when Delivered in HAMC and Contribute to Functional Motor Recovery

To test functional efficacy, behavioral recovery of Et-1 stroke-injured mice was evaluated for NSCs delivered into the stroke lesion site in either HAMC or aCSF versus vehicle-alone and uninjured controls. Animals were evaluated by foot-fault assay 3 days prior to stroke to establish a baseline and 3 days after Et-1-induced stroke to examine the functional deficit. In mice that displayed a functional deficit, NSCs were transplanted 1 day later (i.e., 4 days after stroke), and behavior was evaluated biweekly for 4 weeks (Figure 7A). Mice treated with either aCSF or HAMC alone or NSCs suspended in aCSF showed some, but not significant, recovery relative to the functional deficit observed with stroke injury (at 3 days post-stroke). In contrast, mice transplanted with NSCs delivered in HAMC showed

significant recovery at both 2 and 4 weeks ($p < 0.05$; Figure 7B). Uninjured mice showed no significant difference between time points. Following study completion, the number of animals with surviving cells was evaluated. When NSCs were transplanted in HAMC, 70% (7 of 10) of the animals had surviving cells, whereas only 58% (7 of 12) of the animals transplanted with NSCs in aCSF had surviving cells (Figure S6D). Notwithstanding the functional benefit observed, cells transplanted in HAMC were mostly glial fibrillary acidic protein (GFAP)-positive cells at 4 weeks. Few NeuN+ neurons (Sui et al., 2012) and few Olig2+ oligodendrocytes (Menn et al., 2006) were observed (Figure 7C). Notably, the maximal depth of tissue penetration of NSCs delivered in HAMC was significantly greater than that of NSCs delivered in aCSF both immediately and 4 weeks after transplantation ($p \leq 0.05$; Figure 7D).

DISCUSSION

In this study, we showed that HAMC delivery is critical to both the survival of transplanted RSC-derived rods in retinal dysfunction and NSCs in the stroke-injured brain, demonstrating HAMC's broad applicability with multiple cell types in multiple tissues. Compared to cells transplanted in buffered saline, cells in HAMC were better distributed in the tissue and promoted cell survival and integration—key components for improved behavioral recovery—reflecting remarkable material properties.

The enhanced distribution observed for NSCs delivered in HAMC (versus aCSF) in the brain echoes those observed of RSCs in the retina. This improved cell distribution correlates with greater behavioral recovery, likely reflecting greater cell survival and host tissue integration as a result of improved tissue interaction. The NSC differentiation toward GFAP-positive cells was likely driven by both intrinsic cell properties and transplantation environment. GFAP-positive progenitors have been shown to promote behavioral recovery both in NSC transplantation (Smith et al., 2012) and endogenous stem cell stimulation (Kolb et al., 2007) studies.

The present data implicate the CD44 cell surface receptor to be responsible for the pro-survival effect of HAMC on NSCs and RSC-derived rod photoreceptors in vitro and in vivo. Interactions through CD44 have been shown to be critical to cell survival (Janiszewska et al., 2010), growth, migration (Piao et al., 2013), and differentiation (Ponta et al., 2003). Given the dual functions of CD44 in survival and migration, HAMC may also contribute a pro-migratory effect that dramatically increases RSC-derived rod photoreceptor cell survival in HAMC+AAA treatment in vivo. We attribute the anti-inflammatory and pro-survival effects

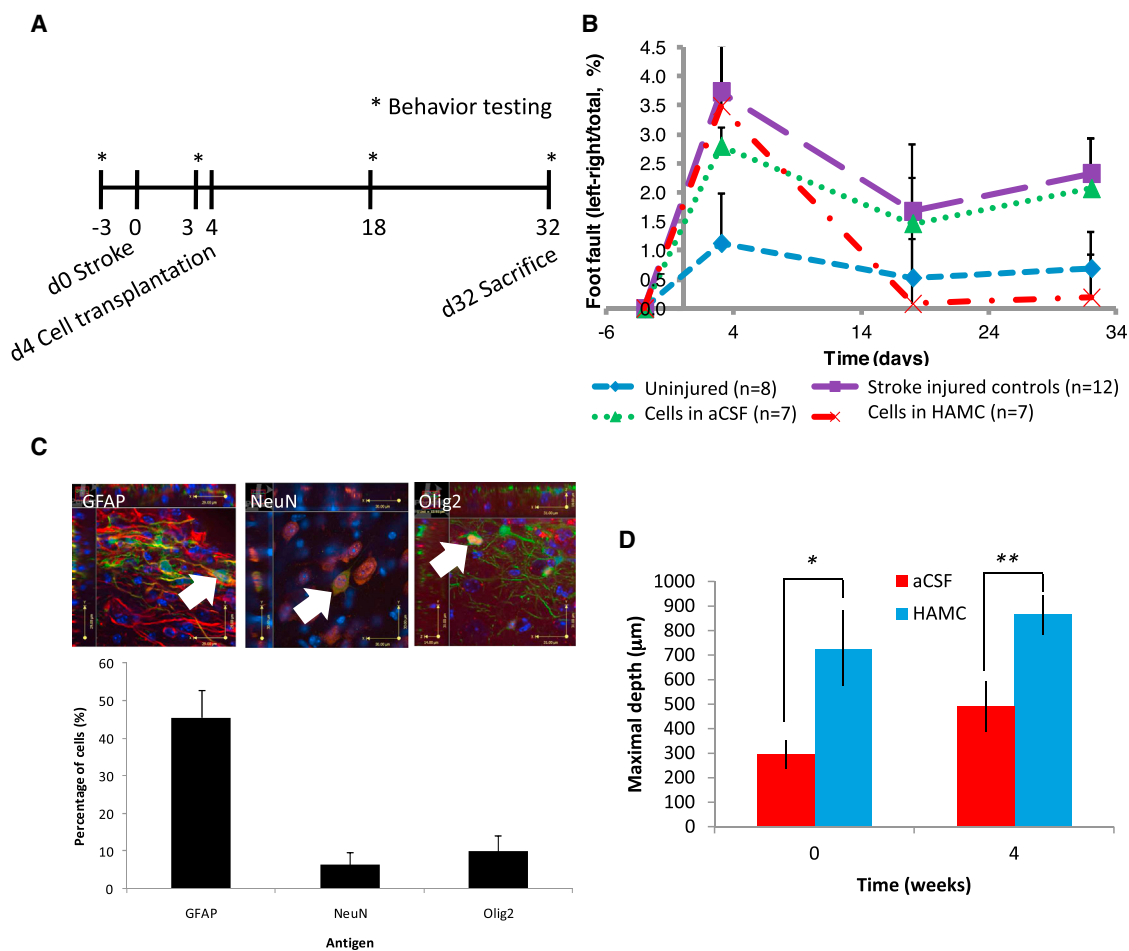


Figure 7. Mice Transplanted with Cells Suspended in HAMC Recover from Stroke Injury

(A) Experimental paradigm shows that mice are tested for the foot fault assay 3 days prior to stroke to establish a baseline and 3 days after stroke to detect the behavioral deficit. At 4 days after stroke, cells are transplanted into the lesion site, and mice are tested 14 and 28 days later (i.e., at 18 and 32 days after stroke, respectively).

(B) At 3 days after injury, foot fault increases significantly in all animal groups except uninjured controls ($n = 8$). At 18 and 32 days after injury, foot fault significantly decreases to pre-injury, baseline values for mice that had NSCs delivered in HAMC ($p < 0.05$, $n = 7$). In contrast, mice that had NSCs delivered in aCSF ($n = 7$) and control mice that had aCSF or HAMC injected without cells ($n = 12$) did not show a significant recovery relative to the functional deficit (i.e., at 3 days). Only mice transplanted with NSCs in HAMC showed behavioral recovery at 14 and 28 days relative to the functional deficit at 3 days.

(C) Representative images of immunohistochemical stained brain tissue, at 28 days after transplantation, show that most of the transplanted NSCs delivered in HAMC are GFAP+ astrocytes, with few NeuN+ neurons and few Olig2+ oligodendrocytes. The majority of transplanted NSCs in HAMC have differentiated into GFAP-expressing astrocytes.

(D) NSCs delivered in HAMC have significantly greater tissue penetration than do those delivered in aCSF at both 0 and 28 days after transplantation ($n = 4$, $p < 0.05$, $p < 0.01$, respectively).

For all graphs, mean \pm SEM are plotted, n independent transplants.

to HA, which is supported by previous studies in the brain (Wang et al., 2013) and spinal cord (Austin et al., 2012) for inflammation.

Previously, immature post-mitotic rod photoreceptors isolated from the early post-natal mouse eye at P4 showed an optimum ability to migrate and integrate into adult host retina (MacLaren et al., 2006). Interestingly, we showed

that mature RSC-derived photoreceptors have the ability to functionally integrate into adult retina. This is consistent with another report suggesting that mature rods isolated from adult mouse eyes can integrate into adult retina and survive with low efficiency (0.16%–0.24%), primarily limited by low cell survival (Gust and Reh, 2011). Our study quantifies the distribution of surviving cells across multiple



host tissue compartments. The engraftment potential of mature rods becomes most noticeable after elimination of specific integration barriers to the neural retina, such as the OLM. The influence of a positive cell survival signal provided by HAMC promotes mature rod survival, resulting in the greatest absolute number of adult stem cell derived rods integrated into neural retina reported to date. These integrated cells demonstrate mature rod morphology and express rod-specific markers *in vivo* as well as contribute to the pupillary light response in this genetically blind mouse model that shows no response to light at baseline. Interestingly, these findings suggest that cell non-autonomous survival factors, provided by a bioactive material, can act differently on cell populations at various developmental stages to encourage integration of one population over another. The mechanisms underpinning the ability of differentiation-stage-specific post-mitotic rod photoreceptors to integrate have yet to be elucidated.

The data demonstrate the benefit of adult RSC- and NSC-based therapies delivered in HAMC for CNS cell replacement therapy. Using an injectable hydrogel delivery strategy to interrogate the mechanism of cell survival, we revealed factors important for successful cell transplantation in both retina and brain. Materials that can address transplantation barriers in a multifaceted approach, as shown with HAMC, will find utility in future cell therapies. Further understanding the interplay of cell survival and integration signals will lead to new designs of clinically relevant strategies for treating CNS diseases for which no regenerative strategies exist.

EXPERIMENTAL PROCEDURES

Animals, Cell Isolation, and Culture

The mice used for isolation and characterization of RSC-derived rods include C57BL/6, *Nrl.gfp* (express GFP in post-mitotic rods), *Actin.gfp* (express GFP in all cells), and *Pax6α-Cre* (Pax6 is enriched in RSCs). Experimental procedures were approved by the Animal Care Committee at the University of Toronto. RSCs were derived from the ciliary epithelium (CE) of adult mice (minimum 6 weeks old). Cells were plated in serum free media (SFM) on non-adherent tissue culture plates (Nunc; Thermo Fisher Scientific) at a clonal density of 20 cells/ μ L. Details on differentiation protocols, survival studies, real-time qRT-PCR, and immunostaining are provided in the [Supplemental Experimental Procedures](#).

Retinal Cell Transplantation, Histology, and Pupillary Light Response

Subretinal transplantation was performed using a trans-scleral approach. *Actin.gfp* RSC-derived cells were chosen as the donor population because of their high survival *in vitro* and the intensity of the actin-driven transgene. Cells were counted (ImageJ) in each of three compartments: neural retina, subretinal space, and RPE. Details can be found in the [Supplemental Experimental Procedures](#).

Mouse NSC Isolation, Culture, and HAMC Preparation

NSCs were isolated from the forebrain subependyma of adult (6- to 8-week) eYFP mice. Details of cell preparation, culture, and HAMC suspension can be found in the [Supplemental Experimental Procedures](#).

Cell Transplantation into Brain

All transplantations were carried out within a 6-hr time window of cell preparation. Control animals were injected with aCSF or HAMC alone without any cells. Two controls were done: (1) stroke-injured animals had the identical volume of aCSF injected, and (2) uninjured animals were left untreated. Details of transplantation technique and histologic and immunocytologic analyses can be found in the [Supplemental Experimental Procedures](#).

Behavioral Analysis

Behavior testing occurred weekly, beginning 3 days prior to stroke. Foot faults were reported as percentage slippage calculated by [(contralateral slips – ipsilateral slips) / total forepaw steps] \times 100. Foot fault was normalized for each mouse to its pre-stroke value. Details can be found in the [Supplemental Experimental Procedures](#).

Cell Counts and Statistics

Actin.gfp+ RSC-derived rods were counted as “integrated” if the whole cell body was correctly located within the neural retina or the subretinal space or was adherent to the RPE layer. Cells were counted if they displayed a nucleus completely surrounded by GFP. All eyes that contained more than one GFP+ cell were included in statistical analysis. All cell counts and pooled data are presented as averages with SEM. Significance was noted for *p* values less than 0.05. Details on statistical methods are provided in the [Supplemental Experimental Procedures](#).

SUPPLEMENTAL INFORMATION

Supplemental Information includes Supplemental Experimental Procedures and six figures and can be found with this article online at <http://dx.doi.org/10.1016/j.stemcr.2015.04.008>.

AUTHOR CONTRIBUTIONS

B.G.B. and M.J.C. designed and performed the RSC and NSC experiments, respectively, and collected and assembled the data. L.D. performed qRT-PCR analysis and assisted with transplantation in the retina, and B.L.K.C. performed *Pax6α-Cre* into *Z/EG* fusion control experiments. All authors were involved with concept, design, data analyses, and manuscript writing.

ACKNOWLEDGMENTS

We thank members of the Morshead, van der Kooy, and Shoichet groups for helpful discussion. Anand Swaroop kindly provided the *Nrl.gfp* mouse strain, and Samer Hattar kindly provided TKO mice. We thank Samantha Yammine, Vincent Huynh, and Shannon Sproul for assistance with behavioral analysis. B.G.B. holds a CIHR Doctoral Canada Graduate Scholarship and McLaughlin Centre Graduate Fellowship. M.J.C. holds a Mitacs



Elevate post-doctoral fellowship and thanks the Stem Cell Network for financial support. This work was supported in part by the CIHR, the Heart and Stroke Foundation, the NIH (R01 EY015716), the Foundation Fighting Blindness (FFB) Canada/Kreml Foundation, the McEwen Centre for Regenerative Medicine, and the Ontario Research Foundation. The authors declare no competing financial interests yet acknowledge that a patent has been issued for HAMC in cell delivery.

Received: December 9, 2014

Revised: April 17, 2015

Accepted: April 17, 2015

Published: May 14, 2015

REFERENCES

- Akimoto, M., Cheng, H., Zhu, D., Brzezinski, J.A., Khanna, R., Filippova, E., Oh, E.C.T., Jing, Y., Linares, J.-L., Brooks, M., et al. (2006). Targeting of GFP to newborn rods by *Nrl* promoter and temporal expression profiling of flow-sorted photoreceptors. *Proc. Natl. Acad. Sci. USA* *103*, 3890–3895.
- Austin, J.W., Kang, C.E., Baumann, M.D., DiDiodato, L., Satkunendrarajah, K., Wilson, J.R., Stanisz, G.J., Shoichet, M.S., and Fehlings, M.G. (2012). The effects of intrathecal injection of a hyaluronan-based hydrogel on inflammation, scarring and neuro-behavioural outcomes in a rat model of severe spinal cord injury associated with arachnoiditis. *Biomaterials* *33*, 4555–4564.
- Ballios, B.G., Cooke, M.J., van der Kooy, D., and Shoichet, M.S. (2010). A hydrogel-based stem cell delivery system to treat retinal degenerative diseases. *Biomaterials* *31*, 2555–2564.
- Ballios, B.G., Clarke, L., Coles, B.L., Shoichet, M.S., and Van Der Kooy, D. (2012). The adult retinal stem cell is a rare cell in the ciliary epithelium whose progeny can differentiate into photoreceptors. *Biol. Open* *1*, 237–246.
- Baumann, M.D., Kang, C.E., Tator, C.H., and Shoichet, M.S. (2010). Intrathecal delivery of a polymeric nanocomposite hydrogel after spinal cord injury. *Biomaterials* *31*, 7631–7639.
- Chaitin, M.H., Wortham, H.S., and Brun-Zinkernagel, A.-M. (1994). Immunocytochemical localization of CD44 in the mouse retina. *Exp. Eye Res.* *58*, 359–365.
- Demontis, G.C., Aruta, C., Comitato, A., De Marzo, A., and Marigo, V. (2012). Functional and molecular characterization of rod-like cells from retinal stem cells derived from the adult ciliary epithelium. *PLoS ONE* *7*, e33338.
- Gupta, D., Tator, C.H., and Shoichet, M.S. (2006). Fast-gelling injectable blend of hyaluronan and methylcellulose for intrathecal, localized delivery to the injured spinal cord. *Biomaterials* *27*, 2370–2379.
- Gust, J., and Reh, T.A. (2011). Adult donor rod photoreceptors integrate into the mature mouse retina. *Invest. Ophthalmol. Vis. Sci.* *52*, 5266–5272.
- Hattar, S., Lucas, R.J., Mrosovsky, N., Thompson, S., Douglas, R.H., Hankins, M.W., Lem, J., Biel, M., Hofmann, F., Foster, R.G., and Yau, K.W. (2003). Melanopsin and rod-cone photoreceptive systems account for all major accessory visual functions in mice. *Nature* *424*, 76–81.
- Inoue, T., Coles, B.L., Dorval, K., Bremner, R., Bessho, Y., Kageyama, R., Hino, S., Matsuoka, M., Craft, C.M., McInnes, R.R., et al. (2010). Maximizing functional photoreceptor differentiation from adult human retinal stem cells. *Stem Cells* *28*, 489–500.
- Janiszewska, M., De Vito, C., Le Bitoux, M.A., Fusco, C., and Stamenkovic, I. (2010). Transportin regulates nuclear import of CD44. *J. Biol. Chem.* *285*, 30548–30557.
- Klassen, H., Sakaguchi, D.S., and Young, M.J. (2004). Stem cells and retinal repair. *Prog. Retin. Eye Res.* *23*, 149–181.
- Kolb, B., Morshead, C., Gonzalez, C., Kim, M., Gregg, C., Shingo, T., and Weiss, S. (2007). Growth factor-stimulated generation of new cortical tissue and functional recovery after stroke damage to the motor cortex of rats. *J. Cereb. Blood Flow Metab.* *27*, 983–997.
- Lamba, D.A., Gust, J., and Reh, T.A. (2009). Transplantation of human embryonic stem cell-derived photoreceptors restores some visual function in *Crx*-deficient mice. *Cell Stem Cell* *4*, 73–79.
- Ma, J., Kabiell, M., Tucker, B.A., Ge, J., and Young, M.J. (2011). Combining chondroitinase ABC and growth factors promotes the integration of murine retinal progenitor cells transplanted into *Rho(-/-)* mice. *Mol. Vis.* *17*, 1759–1770.
- MacLaren, R.E., Pearson, R.A., MacNeil, A., Douglas, R.H., Salt, T.E., Akimoto, M., Swaroop, A., Sowden, J.C., and Ali, R.R. (2006). Retinal repair by transplantation of photoreceptor precursors. *Nature* *444*, 203–207.
- Menn, B., Garcia-Verdugo, J.M., Yachine, C., Gonzalez-Perez, O., Rowitch, D., and Alvarez-Buylla, A. (2006). Origin of oligodendrocytes in the subventricular zone of the adult brain. *J. Neurosci.* *26*, 7907–7918.
- Morshead, C.M., Reynolds, B.A., Craig, C.G., McBurney, M.W., Staines, W.A., Morassutti, D., Weiss, S., and van der Kooy, D. (1994). Neural stem cells in the adult mammalian forebrain: a relatively quiescent subpopulation of subependymal cells. *Neuron* *13*, 1071–1082.
- Mothe, A.J., Tam, R.Y., Zahir, T., Tator, C.H., and Shoichet, M.S. (2013). Repair of the injured spinal cord by transplantation of neural stem cells in a hyaluronan-based hydrogel. *Biomaterials* *34*, 3775–3783.
- Nakagomi, N., Nakagomi, T., Kubo, S., Nakano-Doi, A., Saino, O., Takata, M., Yoshikawa, H., Stern, D.M., Matsuyama, T., and Taguchi, A. (2009). Endothelial cells support survival, proliferation, and neuronal differentiation of transplanted adult ischemia-induced neural stem/progenitor cells after cerebral infarction. *Stem Cells* *27*, 2185–2195.
- Pearson, R.A., Barber, A.C., Rizzi, M., Hippert, C., Xue, T., West, E.L., Duran, Y., Smith, A.J., Chuang, J.Z., Azam, S.A., et al. (2012). Restoration of vision after transplantation of photoreceptors. *Nature* *485*, 99–103.
- Piao, J.H., Wang, Y., and Duncan, I.D. (2013). CD44 is required for the migration of transplanted oligodendrocyte progenitor cells to focal inflammatory demyelinating lesions in the spinal cord. *Glia* *61*, 361–367.



- Ponta, H., Sherman, L., and Herrlich, P.A. (2003). CD44: from adhesion molecules to signalling regulators. *Nat. Rev. Mol. Cell Biol.* 4, 33–45.
- Rattner, A., Smallwood, P.M., Williams, J., Cooke, C., Savchenko, A., Lyubarsky, A., Pugh, E.N., and Nathans, J. (2001). A photoreceptor-specific cadherin is essential for the structural integrity of the outer segment and for photoreceptor survival. *Neuron* 32, 775–786.
- Sarthy, V., Hoshi, H., Mills, S., and Dudley, V.J. (2007). Characterization of green fluorescent protein-expressing retinal cells in CD 44-transgenic mice. *Neuroscience* 144, 1087–1093.
- Smith, E.J., Stroemer, R.P., Gorenkova, N., Nakajima, M., Crum, W.R., Tang, E., Stevanato, L., Sinden, J.D., and Modo, M. (2012). Implantation site and lesion topology determine efficacy of a human neural stem cell line in a rat model of chronic stroke. *Stem Cells* 30, 785–796.
- Sui, Y., Horne, M.K., and Stanić, D. (2012). Reduced proliferation in the adult mouse subventricular zone increases survival of olfactory bulb interneurons. *PLoS ONE* 7, e31549.
- Wang, Y., Cooke, M.J., Sachewsky, N., Morshead, C.M., and Shoi-chet, M.S. (2013). Bioengineered sequential growth factor delivery stimulates brain tissue regeneration after stroke. *J. Control. Release* 172, 1–11.
- West, E.L., Pearson, R.A., Tschernutter, M., Sowden, J.C., MacLaren, R.E., and Ali, R.R. (2008). Pharmacological disruption of the outer limiting membrane leads to increased retinal integration of transplanted photoreceptor precursors. *Exp. Eye Res.* 86, 601–611.